Proceedings of the 21st ICSMGE, Vienna, Austria, 14 – 19 June 2026. Pistrol, Adam & Schweiger (eds.)
Published by: ÖGG, Austrian Society for Geomechanics, Salzburg, Austria, ISBN 978-3-9503898-4-5
https://doi.org/10.53243/ICSMGE2026-1842

Experimental and numerical investigation of concentrated leak erosion in unsaturated slopes

Jack Montgomery, Olaniyi Afolayan, Anna Lancaster, Leila Rahimikhameneh
Auburn University, Auburn, AL, USA, jmontgomery@auburn.edu

ABSTRACT: Concentrated leak erosion (CLE) occurs when subsurface flow is concentrated at an unfiltered exit (e.g., crack, void, macropore), leading to the formation of an eroded pipe (void) within the soil. This process primarily occurs above the water table, where unsaturated conditions control both the progression of erosion and the stability of the void. In dams and levees, the erosion can continue until the void reaches the impounded water, at which point a breach is likely to develop. A similar process is also observed in hillslopes, where the term soil piping is more commonly used, and the collapse of these pipes can lead to landslide initiation. Current methods to evaluate CLE do not explicitly consider the unsaturated properties of the soil and rely primarily on empirical models to determine the likelihood of erosion occurring and progressing. This study employed an integrated program of large-scale experiments and numerical modeling to understand how CLE develops in unsaturated slopes and to identify the impact of changes in soil properties and suction on void stability. The experiments were performed by constructing model slopes with small pre-existing voids to initiate the erosion process. Instrumentation was used to monitor changes in water content and suction at different points within the slope. The experiments demonstrated that an open pipe can act as a drain, leading to higher suction in the slope, whereas collapsed pipes could result in a rapid loss of suction and slope failure. Erosion simulations were used to understand the observations of void enlargement and collapse. The results demonstrate that it is critical to consider both erodibility and collapse due to loss of suction to understand the growth of voids in unsaturated slopes. The results of this study are now being utilized to develop new approaches for evaluating CLE in unsaturated soils.

KEYWORDS: Concentrated leak erosion, unsaturated soil mechanics, slope stability, internal erosion.

1 INTRODUCTION

Internal erosion is a critical failure mechanism in embankments and slopes, responsible for approximately 46% of embankment dam failures globally (Fell et al., 2004; Foster et al., 2000; Richards & Reddy, 2007). This process involves the erosion of soil particles by seepage flow, leading to lateral and downward migration of material (Crosta & Di Prisco, 1999; Prasomsri & Takahashi, 2020; Williamson et al., 2015). Internal erosion can be difficult to detect in the early stages, making it a particularly dangerous failure mode for dams and levees (Robbins & Griffiths, 2018). The internal erosion process generally progresses through four phases: initiation, continuation, progression, and failure (Fell et al., 2004). During initiation, erosion begins at a specific location. In the continuation phase, eroded particles are transported away from the initiation point. The progression phase involves the expansion of the erosion zone, which can potentially lead to the formation of an eroded pipe or cavity. Finally, the failure phase occurs when the erosion has progressed to a point where the structure can no longer maintain its integrity.

Internal erosion encompasses several distinct mechanisms, including concentrated leak erosion (CLE), contact erosion, backward erosion piping, and internal instability (suffusion and suffosion) (Bonelli and Nicot, 2013; Fell & Fry, 2007; Richards & Reddy, 2007; Robbins & Griffiths, 2018). While these erosion types are commonly associated with dams and levees, CLE has also been linked to landslides (Figure 1), debris flows, streambank failures, and gully formation (Faulkner, 2013; Uchida et al., 2001; Wilson, 2011). While significant research has been conducted on backward erosion piping and internal instability, the CLE process remains highly uncertain. Few approaches have been developed to evaluate its effects despite CLE being one of the most common forms of internal erosion.

CLE in slopes can create pathways for preferential flow, which can substantially impact the hydrology and stability of the slope (Kosugi et al., 2004; Nimmo, 2012). These preferential flow paths (voids) influence the pore pressure propagation and slope stability either through enhanced drainage when paths remain open, which improves slope stability, or through increased pore pressure when voids collapse, which poses a stability risk (Shao et al., 2015; Wilson & Fox, 2013; Uchida et al., 2001). The relationship between internal erosion and slope stability remains poorly understood, and further research is necessary to develop models that account for the influence of internal erosion on stability.

Figure 1. Photograph of the soil pipe outlet at a landslide site in West Alabama. The eroded sand can be seen below the glove at the pipe outlet.

This study used physical models to explore the progression of CLE in an unsaturated slope, including the growth and collapse of eroded voids (referred to as soil pipes in this study). The experimental results presented herein, along with those documented by Afolayan et al. (2025a, b, c), demonstrate that open voids can act as a drain, increasing the stability of the slope, while collapsed voids can lead to a rapid loss of suction and slope failure. Erosion simulations were used to understand the observations of void enlargement and collapse. The results demonstrate that it is critical to consider both erosion and collapse due to loss of suction to understand the growth of voids in unsaturated slopes. The results of this study are now being utilized to develop new approaches for evaluating CLE in unsaturated soils.

2 EXPERIMENTAL PROGRAM

2.1 *Model Design*

The experimental design focused on understanding the behavior of an eroded pipe that formed near the toe of a potentially unstable slope (Figure 2). For these experiments, a clayey sand (SC) slope was constructed over an impermeable layer (created using EPS foam coated with sanded epoxy, as shown in Figure 3). A 1.2 cm void was created using a metal rod that was removed before testing. This initial void (representing a macropore or other defect) was located at the interface between the clayey sand slope and the impermeable layer. This is consistent with field observations that often find pipes developing at an interface with an impermeable soil horizon or other low-permeability layer (Bernatek-Jakiel & Poesen, 2018). A standpipe was placed on the upslope side of the model, allowing flow to be introduced directly into the open void. The maximum height of the slope was 45 cm, with a base angle of approximately 11°. Volumetric water content (Teros 10/11) and suction sensors (Teros 21) were placed at different locations in the slope (Figure 2).

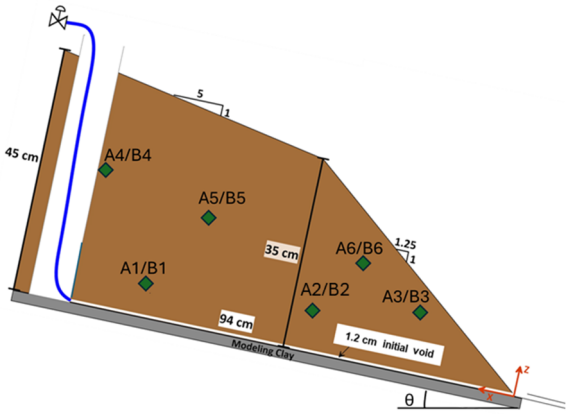

Figure 2. Cross-section of the model showing the sensors' location. The locations of the sensors (A1/B1 – A6/B6) are indicated by green diamonds. The width of the model (y-direction) is 120 cm.

Figure 3. The container for the experiments was created using EPS foam blocks coated with sanded epoxy. A rigid wooden frame was used to hold the EPS in place (not shown in the photo).

2.2 *Model Construction*

The model slope was constructed using locally sourced fill material from Auburn, Alabama, USA. The soil was passed through a No. 4 sieve (4.75 mm opening) to eliminate large aggregates and other debris. The soil was a clayey sand (SC) according to the USCS soil classification method, with a D_{50} of 0.5 mm, a fines content of 21.5%, a liquid limit of 67%, and a plasticity index of 20%. Standard Proctor compaction testing showed an optimum water content of 13% and a maximum dry density of 1.90 Mg/m^3. Further details on the soil properties are provided by Afolayan et al. (2025a).

After positioning the metal rod on the foam block, the soil was mixed to a gravimetric water content (GWC) of approximately 9%. The soil was then placed in 2.5 cm lifts and compacted using a hand tamper to achieve the desired relative compaction (either 80% for the loose slope or 93% for the dense slope). To ensure accurate placement of the lifts, reference marks were made on the sides of the container at the desired thickness. A temporary board was positioned at the front of the container to provide shoring and support for the soil during compaction. Sensors were placed at the desired locations during model construction, and care was taken not to damage the sensors or wires while placing subsequent lifts. Following compaction, the temporary board was removed and the surface of the slope was shaped to achieve the final profile (Figure 2). A photo of one of the completed slopes is shown in Figure 4.

Figure 4. Completed slope after pipe removal, but before testing. The standpipe is shown at the top of the slope along with the tube used to introduce flow into the pipe.

2.3 *Testing Procedure*

The objective of the test was to observe the behavior of the eroded pipe and the slope during subsurface flow. To simulate subsurface seepage, water was introduced into the standpipe and allowed to flow out from the toe, where it was collected and recirculated. A gate valve was used to establish and maintain a constant flow rate of approximately 130 mL/s. Tests were terminated either upon slope failure or after no further erosion was observed. Video recordings were used to identify key events during the test, such as seepage emergence at the toe, changes in flow that might indicate blockage of the pipe, and any slope movements or cracking. These observations were combined with sensor measurements to understand the slope response. All experimental data, including video recordings, are available from Afolayan et al. (2025a).

3 EXPERIMENTAL RESULTS

This paper presents results from three tests that are part of a larger series of tests by Afolayan et al. (2025a). The basic test parameters are shown in Table 1 using the same naming convention as Afolayan et al. (2025a).

Table 1. Parameters for slope experiments.

Parameter	Relative Compaction	GWC (%)	Final State of Slope
Test M3-Wide	80%	9.1	Stable
Test M4-Wide	80%	8.6	Unstable
Test D3-Wide	93%	9.3	Stable-

In Test M3-Wide, the slope was compacted to a relative compaction (RC) of 80% and a GWC of 9.1%. The sensor responses are shown in Figure 5. Seepage was observed at the toe approximately 2 minutes and 38 seconds after starting flow into the standpipe. VWC sensor A1 (located closest to the standpipe) showed an immediate response, indicating that seepage was entering the slope; however, a collapse likely occurred in the pipe, resulting in a blockage of flow. By the time the blockage was cleared, suction sensors B1, B2, and B4 were all showing near-zero suction, and the corresponding VWC sensors were all near or above 35%. Once the flow exited the pipe, the pipe began acting as a drain, resulting in a reduction in the VWC of all sensors except A3 (Figure 5a). The slope remained stable throughout the test, although the void continued to enlarge, reaching a final width of approximately 30 cm and a height of approximately 15 cm.

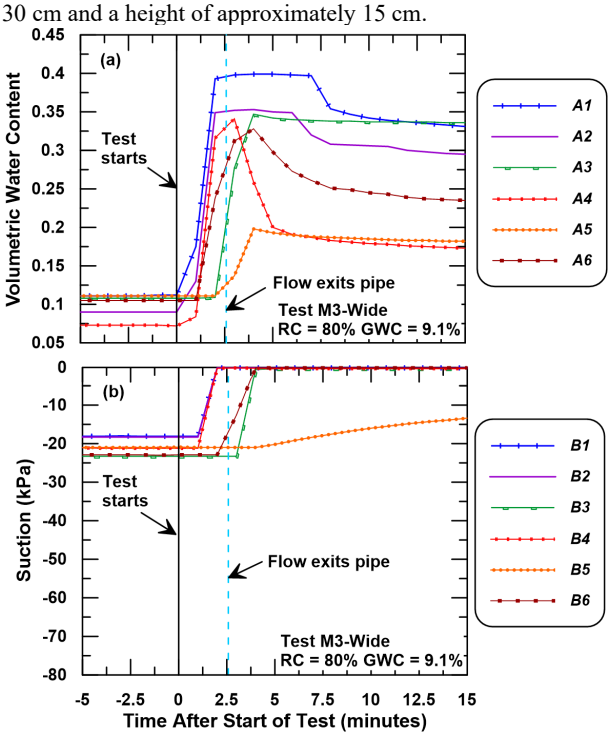

Figure 5. Volumetric water content and suction measurements for the six pairs of sensors used in Test M3-Wide. Sensor locations are shown in Figure 2.

Figure 6 shows a series of still images extracted from the video recording showing how the void enlarged over the first few minutes of the test. Figure 6a shows the void approximately 1 minute after seepage began flowing out of the pipe. The growth of the void up to this point occurred at a fairly regular rate. Figure 6b shows a sudden collapse of the roof over the void four seconds after Figure 6a. This collapse was cleared over the next 15 seconds by the flow through the pipe, leaving a newly enlarged pipe (Figure 6c). The collapse and stabilization of the pipe corresponded with the loss of suction in sensors B3 and B6 (Figure 5b). This loss of suction led to the arch becoming unstable and collapsing until a new stable arch could form higher in the slope. The new arch (Figure 6c) was approximately 18 cm wide and 12 cm tall. This demonstrates that the growth of voids in unsaturated slopes can occur through both erosion (commonly considered in CLE models) and the local collapse of the roof or sides of the void. The effects of suction on arch stability are explored further in the next section.

Test M4-Wide was performed with the same target density as Test M3-Wide, but with a drier soil (8.6% GWC). Afolayan et al. (2023) found, from bench-scale tests on the same soil, that 9% GWC tended to be the boundary between slopes that formed a stable void and those that were more likely to collapse. The sensor responses for M4-Wide are shown in Figure 7. Seepage did not exit the pipe until almost four minutes after the test began. Sensors A1 and A2 showed a rapid increase in VWC, indicating the initial void was blocked and took longer to clear than in Test M3-Wide. After the flow emerged from the pipe, the pipe began to erode and enlarge, proceeding at an approximately constant rate for about one and a half minutes. After this point, the pipe began to enlarge rapidly through a series of collapses, eventually reaching a height of approximately 30 cm. At that point, the slope became unstable, with a large crack forming, and a complete slope failure occurred approximately 7 minutes and 51 seconds after the test began.

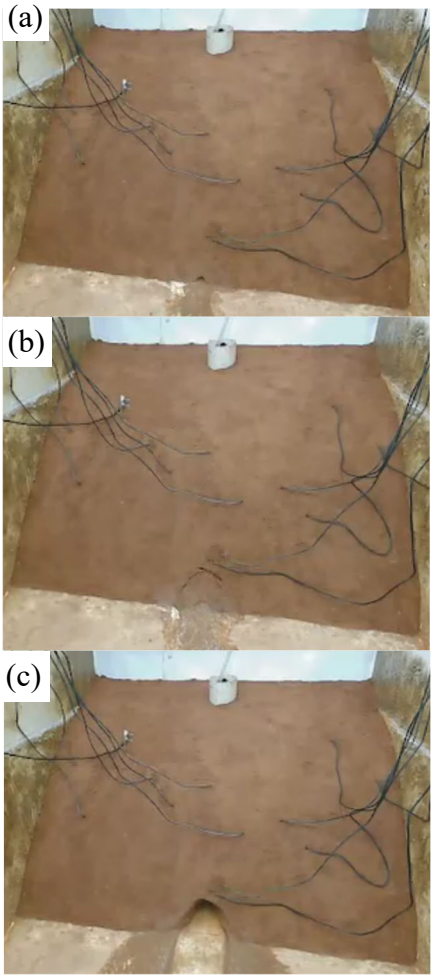

Figure 6. Photos of Test M3-Wide showing (a) initial enlargement of the void (3:26 after start of test), (b) a collapse of the roof over the void (3:30 after start of test), and (c) formation of a new stable arch after the collapsed material was cleared from the void (3:50 after start of test).

Comparing the VWC and suction responses between Tests M3-Wide and M4-Wide offers some insight into these very different behaviors (stability versus complete collapse). In Test M3-Wide, the initial blockages were quickly cleared, allowing the eroded pipe to act as a drain and increasing the stability of the slope. There was some initial loss of suction in the sensors closest to the pipe, but sensor B5 (located in the upper part of the slope) maintained a suction of approximately 15 kPa at the end of the test, which was enough to support the roof of the eroded pipe and to maintain stability of the slope. In Test M4-Wide, the blockages were too large to be quickly cleared, and the VWC sensors continued to rise until the slope began to fail. All six sensors showed near-zero suction at the end of the test.

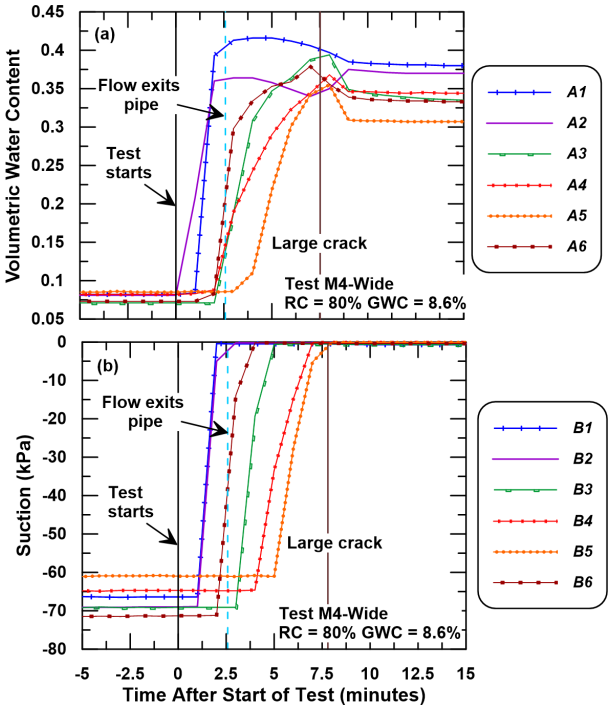

Figure 7. Volumetric water content and suction measurements for the six pairs of sensors used in Test M4-Wide.

Test D3-Wide was constructed at a similar GWC to Test M3-Wide (9.3%), but at an RC of approximately 93%. Water began flowing from the pipe exit immediately after the test started. Sensors A1/B1, A2/B2, and A3/B3 responded during the test (Figure 8), but all three sensor pairs were delayed compared with the other two tests. The remaining sensors did not exhibit significant changes during the test. The slope stayed stable with no observable external movement, although the void did enlarge through erosion. No collapses were observed, indicating that the dense soil maintained sufficient suction to support the roof over the pipe and ensure stability of the slope.

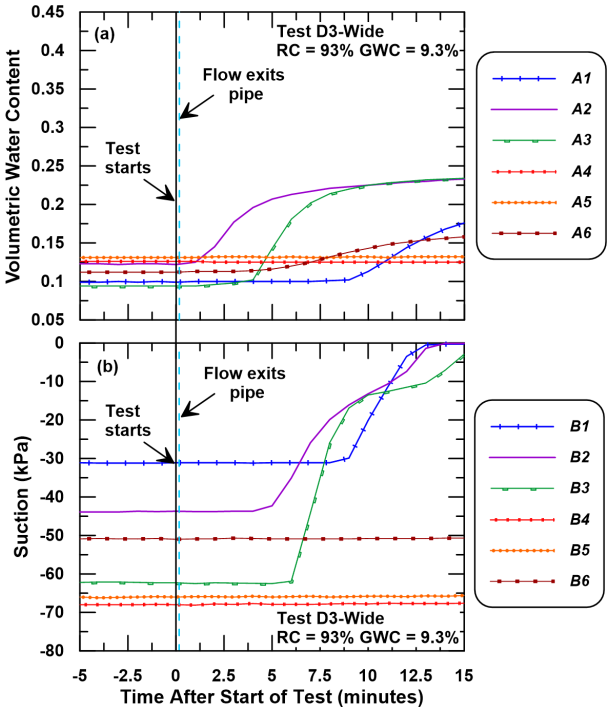

Figure 8. Volumetric water content and suction measurements for the six pairs of sensors used in Test D3-Wide.

4 NUMERICAL ANALYSIS

To better understand the observations from these three experiments, a pair of simulations were performed to estimate how the initial 1.2 cm void would grow with time due to the seepage flow. The simulation approach is similar to those used by Bonelli et al. (2006), Xu and Zhang (2013) and Wu (2016) to model CLE in embankments. In the current study, the pipe is treated as a uniform semi-circle along its length, so the simulations are essentially one-dimensional (1D). The simulations currently only account for void growth due to erosion, but the importance of also considering void stability is discussed next. All simulations in this study were performed using Python (v3.12). Several properties had to be estimated for this process. A Manning's roughness coefficient (n) of 0.04 was used to account for the irregular walls and rough bottom of the pipe. The erodibility (E_τ) and critical shear stress (τ_c) were estimated based on the equations proposed by Briaud et al. (2019, Tables 91 and 96). The properties used in the simulation are shown in Table 2.

Table 2. Parameters for erosion simulations.

Relative Compaction	Critical Shear Stress (τ_c) Pa	Erodibility (E_τ) $m^3/N{\cdot}s$
80%	0.5	5.0E-5
93%	0.5	1.9E-5

The basic steps used to simulate the erosion process over time were:

(1) The initial void was assumed to be 1.2 cm tall and open along its length. Hence, the simulations only consider the portion of time after flow emerges from the pipe (ignoring any initial blockage). The initial height of the water in the standpipe was assumed to be at the top of the void. A timestep (Δt) of two seconds was used, but other values did not change the results.

(2) A new water height was estimated based on the inflow into the standpipe (130 mL/s) and the flow rate through the pipe. The flow rate (Q) was calculated using the orifice flow equation (as described by Wu 2016) if the water level was at or above the height of the pipe, or Manning's open channel flow equation if the height of the water was below the top of the pipe.

(3) The average flow velocity (Q/A) was used to estimate the shear stress on the walls (τ_w) of the pipe using the approach suggested by Guo (2015).

(4) The shear stress on the walls of the pipe was compared with the critical shear stress. If the applied shear stress exceeded the critical value, the soil was assumed to erode from the sides of the pipe. The width of the pipe (W_{pipe}) was increased according to Equation 1. The geometry of the pipe was assumed to be a semicircle, so any increase in width also led to an increase in height.

$$\Delta W_{pipe} = 2\left(E_\tau(\tau_w - \tau_c)\right)\Delta t \quad (1)$$

(5) Steps 2 – 4 were repeated with the new pipe geometry for the next timestep

The analysis approach described above does not consider the effects of suction or stability of the eroded void, but collapse was an important mechanism for the tests performed at 80% RC. Guo and Zhou (2013) explored the formation of stable arches in granular materials with small apparent cohesions. The

equation for the critical width (B_{crit}) of an arch proposed by Guo and Zhou (2013) is shown in Equation 2.

$$B_{crit} = \frac{5.14c(tanh(3\varphi))^{3.5}}{\rho g} sin\left(\frac{\pi}{4}+\frac{\varphi}{2}\right) \quad (2)$$

Where c is the apparent cohesion, φ is the friction angle (34° for this analysis), ρ is the density of the soil, and g is gravity. The apparent cohesion can be estimated based on the suction stress (σ_s) using Equation 3 (Lu and Likos 2013).

$$c = -\sigma_s tan(\varphi) \quad (3)$$

Equations 2 and 3 are used in the next section to estimate how large the void can become before collapse would be expected.

4.1 *Analysis Results*

The simulation approach described in the previous section was applied to the tests presented in Section 3. The simulation results are shown in Figure 9 along with the estimated height of the eroded pipe from the three tests. Note that this figure shows results starting from the time that flow was observed at the pipe exit and so does not consider the initial blockages.

There is relatively good agreement between the simulation results and the observations from Test D3-Wide, which did not experience any significant pipe collapse. For Test M3-Wide and M4-Wide, there is good agreement for the first minute after flow emerges, but then the experimental observations show more rapid pipe growth than would be suggested by erosion alone. This deviation is attributed to the local collapses of the pipe's sides and roof that were observed during the experiments.

Lines of critical arch height (assumed to be half of the arch width from equation 2) are shown in Figure 9 for different levels of suction stress. These critical heights mark the boundary between stability and collapse for a given suction stress. For a suction stress of 1 kPa, the maximum height of the pipe is approximately 7 cm. This increases to 15 cm for a suction stress of 2 kPa and to 31 cm for a suction stress of 4 kPa. These results help explain how a new stable arch could form after an initial pipe collapse, as the suction stress is higher further away from the pipe. As the collapse reaches these zones with higher suction, the soil can support a larger arch, allowing a new roof to form over the enlarged pipe.

This pattern of collapse and stabilization was observed in Test M3-Wide (Figure 6b and 6c), as the upper part of the slope maintained a higher suction (Figure 5). This higher suction was sufficient for the pipe to stabilize at a height of 12 cm, and no further erosion was observed as the velocity of the water in the pipe was then too low to cause erosion. For Test M4-Wide, the pipe temporarily stabilized at approximately 16 cm and then again at 30 cm; however, the lower suction in the upper parts of the slope was insufficient for the arch to fully stabilize, resulting in failure of the slope. For Test D3-Wide, the suction remained high throughout the test, and so no collapse occurred.

Coupling this analysis of stable voids with erosion simulations is critical for improving current analysis methods for CLE in slopes and embankments. Integrating these two analyses requires estimating how the suction stress varies within the slope, both as a function of distance from the pipe and time. The authors are currently working on this topic and plan to expand on the modeling approach discussed in this study in the future.

5 CONCLUSIONS

Concentrated leak erosion is a critical failure mode for dams and levees and has also been linked to landslides (Figure 1), debris flows, streambank failures, and gully formation. Current approaches for estimating the progression of CLE primarily focus on erosion, but it is also important to consider the response of the unsaturated soils surrounding the eroded void (pipe). This study used physical models to investigate how CLE impacts the VWC and suction in a slope with an initial void. Controlled seepage was introduced into the void, which then began to erode. The experiments using the looser soil showed that the pipe may have some initial blockage that can lead to increases in VWC and decreases in suction around the pipe. The denser slope did not show any collapses or blockages. All three experiments showed the pipe initially grew through erosion. The two tests with the looser soil also showed that local collapse of the roof and/or sides of the pipe could rapidly increase the size of the pipe. When the pipe was blocked, the VWC increased and the suction decreased. For test M4-Wide, the loss of suction led to a slope failure. When the pipe was open, it acted as a drain, decreasing the VWC in the slope and increasing stability. Similar observations were made by Afolayan et al. (2025b) using a smaller model.

A pair of simulations was performed to understand how commonly applied erosion procedures would compare with the observed pipe progression. For the denser slope (Test D3-

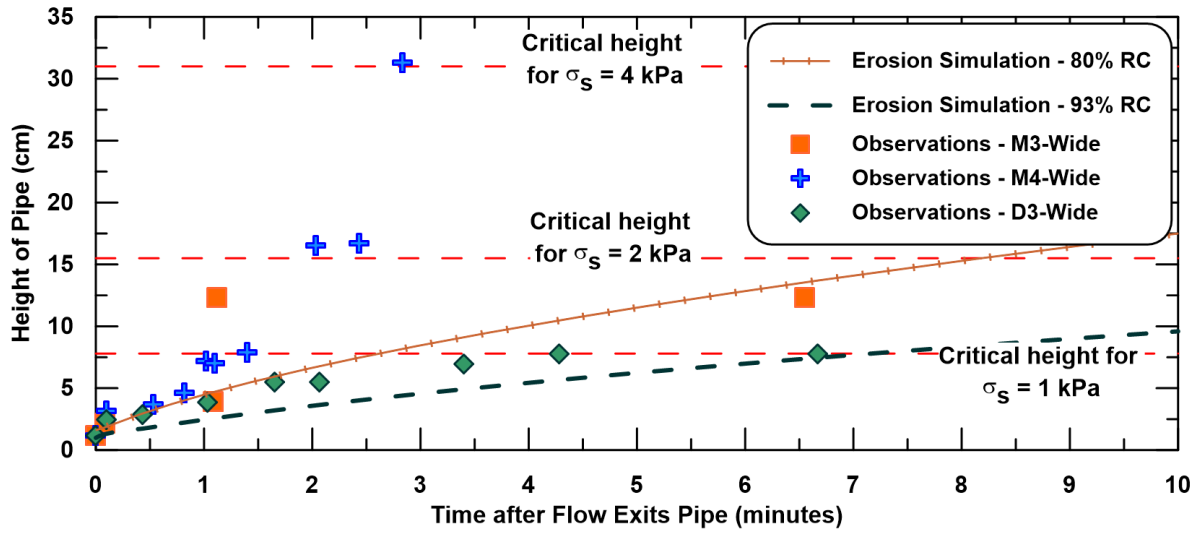

Figure 9. Comparison of observed heights of the eroded pipe with results of the erosion simulations. Critical heights before collapse would be expected to occur are also shown for different suction stresses.

Wide), the simulations were in good agreement. This test did not exhibit any signs of collapse, indicating that the observed pipe enlargement was primarily due to erosion. The analyses were effective in predicting this growth over time. For the other two tests, the simulations initially agreed with the observations but the pipe in the experiments also grew through local collapse of the roof and sides of the pipe. These local collapses were attributed to loss of suction, and this aspect is not captured in current analysis approaches. The stable arch formulation proposed by Guo and Zhou (2013) shows promise in explaining the formation of new stable pipes after a collapse. More work is needed to integrate erosion simulations with arch stability analyses to capture both modes of pipe growth (erosion and collapse).

The current study has only considered a single soil type and two densities, resulting in a limited dataset. The authors have conducted additional experiments (Afolayan et al., 2025a) and plan to apply the analyses described in this study to these experiments in the future. Additional experiments are also planned to investigate other soil types and to explicitly measure both upslope and downslope water levels, thereby refining the hydraulic modeling approach used in this study.

6 ACKNOWLEDGEMENTS

The authors appreciate the support provided by Chukwuma Okafor, Mal Jenkins, India Warren, Evelyn Chavez, Taylor Renfroe, and Lorenzo during the experimental testing. Funding for this work was provided by the National Science Foundation under award number CMMI 2047402, including REU supplements. Any opinions, findings, and conclusions or recommendations are those of the author(s) and do not necessarily reflect the views of the National Science Foundation.

7 REFERENCES

Afolayan, O., McLeod, J. And Montgomery, J. 2023. Effect of Water Content on Internal Erosion of an Unsaturated Slope. Geo-Congress 2023. https://doi.org/10.1061/9780784484654.043

Afolayan, O., Lancaster, A. and Montgomery, J. 2025a. Effects of density and slope angle on internal erosion in an unsaturated clayey sand slope. *Physical Modeling of Internal Erosion and Shallow Landslide Initiation in Unsaturated Slopes*. DesignSafe-CI. https://doi.org/10.17603/ds2-c5sm-1c95

Afolayan, O., Lancaster, A. and Montgomery, J. 2025b. Impact of soil piping on shallow landslide initiation: Experimental Observations. *ESS Open Archive*. DOI: 10.22541/essoar.175195383.36518934/v1

Afolayan, O., Lancaster, A. and Montgomery, J. 2025c. Effect of Matrix Properties and Pipe Characteristics on Internal Erosion in Unsaturated Clayey Sand Slope. *Geosciences*. 2025; 15(10):405. https://doi.org/10.3390/geosciences15100405

Bernatek-Jakiel, A., and Poesen, J. 2018. Subsurface erosion by soil piping: significance and research needs. *Earth-Science Reviews* Vol. 185. Elsevier B.V. https://doi.org/10.1016/j.earscirev.2018.08.006

Briaud, J-L, Shafii, I., Chen, H-C., and Medina-Cetina, Z. 2019. *Relationship Between Erodibility and Properties of Soils*. National Academies of Sciences, Engineering, and Medicine. Washington, DC: The National Academies Press. https://doi.org/10.17226/25470.

Bonelli, S., Brivois, O., Borghi, R., and Benahmed, N. 2006. On the modelling of piping erosion. *Comptes Rendus Mécanique*. 334, 555–559. https://doi.org/10.1016/j.crme.2006.07.003

Bonelli, S. and Nicot, F. 2013. *Erosion in geomechanics applied to dams and levees.* John Wiley and Sons, Inc. DOI:10.1002/9781118577165

Crosta, G., and Prisco, C. D. 1999. On slope instability induced by seepage erosion. *Canadian Geotechnical Journal*, 36(6), 1056–1073.

Faulkner, H. 2006. Piping hazard on collapsible and dispersive soils in Europe. In: Boardman, J., Poesen, J. (Eds.), *Soil Erosion in Europe*. Wiley, Chichester, pp. 537–562. http://dx.doi.org/10.1002/0470859202.

Faulkner, H. 2013. Badlands in marl lithologies: A field guide to soil dispersion, subsurface erosion and piping-origin gullies. *Catena*, 106, 42–53. https://doi.org/10.1016/j.catena.2012.04.005

Fell, R., and Fry, J. 2007. Internal erosion of dams and their foundations. *Selected and Reviewed Papers from the Workshop on Internal Erosion and Piping of Dams and their Foundations, Aussois, France.* 25-27 April 2005. Taylor & Francis. https://doi.org/10.1201/9781482266146

Fitzpatrick, R. W., Boucher, S. C., Naidu, R., and Fritsch, E. 1994. Environmental consequences of soil sodicity. *Soil Research*, 32(5), 1069–1093.

Fell, R., Wan, C. F., and Foster, M. 2004. *Methods for Estimating the Probability of Failure of Embankment Dams by Internal erosion and Piping- Piping through the embankment*. UNICIV Report R-436, University of New South Wales, School of Civil and Environmental Engineering.

Foster, M., Fell, R., and Spannagle, M. 2000. The statistics of embankment dam failures and accidents. *Canadian Geotechnical Journal*, 37, 1000–1024.

Guo, J. 2013. Sidewall and non-uniformity corrections for flume experiments. *Journal of Hydraulic Research.* Vol. 53, No. 2. http://dx.doi.org/10.1080/00221686.2014.971449

Guo, P. and Zhou, S. 2015. Arch in granular materials as a free surface problem. *Int. J. Numer. Anal. Meth. Geomech*. 2013; 37:1048–1065. DOI: 10.1002/nag.1137

Kosugi, K., Uchida, T., and Mizuyama, T. 2004. Numerical calculation of soil pipe flow and its effect on water dynamics in a slope. *Hydrological Processes*, 18(4), 777–789. https://doi.org/10.1002/hyp.1367

Lu, N. and Likos, W. J. 2013. Origin of Cohesion and Its Dependence on Saturation for Granular Media. *Poromechanics V: Proceedings of the Fifth Biot Conference on Poromechanics*. https://doi.org/10.1061/9780784412992.197

Nimmo, J. R. 2012. Preferential flow occurs in unsaturated conditions. *Hydrological Processes.* 26(5). https://doi.org/10.1002/hyp.8380

Prasomsri, J., and Takahashi, A. (2020). The role of fines on internal instability and its impact on undrained mechanical response of gap-graded soils. *Soils and Foundations*, 60(6), 1468–1488. https://doi.org/10.1016/j.sandf.2020.09.008

Richards, K. S., and Reddy, K. R. (2007). Critical appraisal of piping phenomena in earth dams. *Bulletin of Engineering Geology and the Environment*, 66(4), 381–402. https://doi.org/10.1007/s10064-007-0095-0

Robbins, B. A., and Griffiths, D. V. (2018). Internal Erosion of Embankments: A Review and Appraisal. *Rocky Mountain Geo-Conference GPP12*, 61–75

Shao, W., Bogaard, T. A., Bakker, M., and Greco, R. (2015). Quantification of the influence of preferential flow on slope stability using a numerical modelling approach. *Hydrology and Earth System Sciences*, 19(5), 2197–2212. https://doi.org/10.5194/hess-19-2197-2015

Uchida, T., Kosugi, K. N. I., and Mizuyama, T. (2001). Effects of pipeflow on hydrological process and its relation to landslide: A review of pipeflow studies in forested headwater catchments. *Hydrological Processes*, 15(11), 2151–2174. https://doi.org/10.1002/hyp.281

Williamson, T., Hughes, A., Hope, I., Mason, P., Bridle, R., Grubb, K., and Tudor, S. (2015). *Meeting report: ICOLD Annual Meeting and Congress 2015*, Stavanger.

Wilson, G. (2011). Understanding soil-pipe flow and its role in ephemeral gully erosion. *Hydrological Processes*, 25(15), 2354–2364. https://doi.org/10.1002/hyp.7998

Wilson, G. V., and Fox, G. A. (2013). Pore-Water Pressures Associated with Clogging of Soil Pipes: Numerical Analysis of Laboratory Experiments. *Soil Science Society of America Journal*, 77(4), 1168–1181. https://doi.org/10.2136/sssaj2012.0416

Wu, W. (2016). *Introduction to DLBreach–A simplified physically-based dam/Levee breach model*. Clarkson University, NY.

Xu, T., and Zhang, L. (2013). Simulation of piping in earth dams due to concentrated leak erosion. *Geo-Congress 2013: Stability and Performance of Slopes and Embankments III* (pp. 1091-1099).